

Anisotropic optical spectra of $\text{BaCo}_{1-x}\text{Ni}_x\text{S}_2$: Effect of Ni substitution on the electronic structure of the $\text{Co}_{1-x}\text{Ni}_x\text{S}$ plane

K. Takenaka,* S. Kashima, A. Osuka, S. Sugai, Y. Yasui, S. Shamoto,[†] and M. Sato
Department of Physics, Nagoya University, Nagoya 464-8602, Japan

(Received 8 October 2000; published 1 March 2001)

Polarized optical reflectivity is studied in single crystals of $\text{BaCo}_{1-x}\text{Ni}_x\text{S}_2$ over a wide compositional range $0 \leq x \leq 0.28$ from the antiferromagnetic insulating to the paramagnetic metallic phase. BaCoS_2 is a charge-transfer-type Mott insulator with an anisotropic optical gap of about (or less than) 1 eV for $\mathbf{E} \perp c$ (parallel to the CoS plane) and 3.5 eV for $\mathbf{E} \parallel c$ (perpendicular to the CoS plane). Ni substitution for Co has different effects on the in-plane $\sigma_{ab}(\omega)$ and out-of-plane $\sigma_c(\omega)$ conductivities. As the Ni substitution proceeds, a Drude-like peak develops in $\sigma_{ab}(\omega)$ above $x=0.18$, while a mid-infrared absorption band develops and a Drude-like peak is not confirmed in $\sigma_c(\omega)$. This indicates that the two-dimensionality is stronger than predicted from band calculations. However, the mid-infrared spectral weight induced in $\sigma_c(\omega)$ is much larger than that of high- T_c cuprates. This suggests that the charge carriers are not so tightly confined within the plane as in high- T_c cuprates. The looseness of the charge confinement probably originates from a strong interlayer-coupling effect via the $3d_{3z^2-r^2}$ orbital.

DOI: 10.1103/PhysRevB.63.115113

PACS number(s): 71.27.+a, 71.30.+h, 78.20.-e

I. INTRODUCTION

The layered sulfide $\text{BaCo}_{1-x}\text{Ni}_x\text{S}_2$, consisting of $\text{Co}_{1-x}\text{Ni}_x\text{S}$ planes separated by rocksalt BaS blocks, is a strongly correlated quasi-two-dimensional (2D) system.^{1,2} BaCoS_2 , with Co^{2+} in the $(3d)^7$ configuration, is an antiferromagnetic Mott insulator²⁻⁴ (Néel temperature $T_N=310$ K) contrary to the prediction of a metal of band calculations.⁵ The system undergoes a Mott insulator to metal (I-M) transition at $x \sim 0.2$ on substituting Ni for Co.^{2,6} Previous studies suggest the 2D nature of the $\text{Co}_{1-x}\text{Ni}_x\text{S}$ plane^{7,8} and various anomalous behaviors in the metallic phase near the Mott transition, such as a temperature-dependent Hall coefficient, are shared with high-temperature superconducting (high- T_c) cuprates.⁶ The dynamical magnetic properties have also been studied by means of neutron inelastic scattering.⁸⁻¹⁰ The Mott transition is induced also by rather small pressure^{11,12} and an anomalous transition from a high- T antiferromagnetic insulator (AFI) to a low- T paramagnetic metal (PMM) occurs in sulfur-deficient $\text{BaCo}_{1-x}\text{Ni}_x\text{S}_{2-y}$.^{2,13-15} The present sulfide system is a suitable subject for the study of the peculiar physical properties of doped Mott insulators, which is one of the central concerns in current condensed matter physics.

Optical reflectivity study, bridging the gap between dc transport properties and high-energy spectroscopy, is a powerful tool for investigating the electrical properties of conducting carriers as well as the electronic structure in the vicinity of the Fermi level. Therefore, it is expected to reveal the evolution of the electronic structure of $\text{BaCo}_{1-x}\text{Ni}_x\text{S}_2$ and its anisotropic charge transport. Previous work by Kim *et al.* reported the T -dependent far-infrared (far-IR) spectra of the sulfur deficient polycrystalline $\text{BaCo}_{0.9}\text{Ni}_{0.1}\text{S}_{1.9}$ and revealed an anomalous Drude-like response with remarkably small energy width and extremely small spectral weight.¹⁶ However, it is expected that mixing of the anisotropic reflectivities conceals the difference between the in-plane and out-of-plane electronic properties.

We measured the reflectivity $R(\omega)$ spectra of single-crystalline $\text{BaCo}_{1-x}\text{Ni}_x\text{S}_2$ over a wide energy range 0.005–40 eV for both polarizations, parallel ($\mathbf{E} \perp c$) and perpendicular ($\mathbf{E} \parallel c$) to the $\text{Co}_{1-x}\text{Ni}_x\text{S}$ plane. The present experiment has revealed the overall features of the electronic structure as the Ni concentration increases from $x=0$ (AFI) to 0.28 (PMM). The electronic states are reconstructed on a large energy scale at the Mott transition, which is incompatible with the rigid band picture. Based on the present results, we discuss the differences in the electronic states and structure between the present sulfide system and a typical high- T_c cuprate $\text{La}_{2-x}\text{Sr}_x\text{CuO}_4$.

II. EXPERIMENTS

Single crystals of $\text{BaCo}_{1-x}\text{Ni}_x\text{S}_2$ were grown by a self-flux method. The sulfur deficiency in the as-grown crystals was reduced by annealing them at 900 °C in a sealed quartz tube together with polycrystalline $\text{BaCo}_{1-x}\text{Ni}_x\text{S}_2$ which had a prescribed sulfur content. Details of the sample preparation are given elsewhere.^{7,11,17} Typical crystal size was 1.0×1.0 mm² in the (ab) plane and 0.1 mm along the c axis, which was sufficient for optical measurements when we used the microscope designed for the infrared-visible spectrometer.

Near-normal incident reflectivity measurements were made using a Fourier-type interferometer (0.005–2.2 eV), a grating spectrometer (1.2–6.6 eV), and a Seya-Namioka type spectrometer for vacuum-ultraviolet synchrotron radiation (4.0–40 eV) at the Institute for Molecular Science, Okazaki National Research Institutes. As a reference mirror, we used an evaporated Au (far- to near-IR region) and Ag (visible region) film on a glass plate. The experimental error for the reflectivity, ΔR , determined from the reproducibility, is less than 1% for the far-IR to visible region and less than 2% for the ultraviolet to vacuum-ultraviolet region. The reflectivity spectra were measured on surfaces polished by a lapping film with diamond powder of diameter 0.5 μm . For the representative compositions, we also measured the in-plane ($\mathbf{E} \perp c$)

reflectivity on the cleaved surfaces and confirmed that the spectra measured on both the polished and cleaved surfaces are essentially the same.

For quantitative discussion, we deduced the optical conductivity $\sigma(\omega)$ from the measured $R(\omega)$ data via a Kramers-Kronig (KK) transformation. In order to use this transformation, appropriate extrapolations are necessary. Since the experiment covers the energy region up to 40 eV, which includes contributions from almost all the valence electrons in the material, our extrapolation to the higher-energy region (we assumed $R \propto \omega^{-4}$) does not affect $\sigma(\omega)$ in the energy region of interest. Below 5 meV, we made the extrapolation in the following manner. For both polarizations, constant reflectivity was assumed for the insulating compounds ($x = 0-0.14$) while Hagen-Rubens (HR) reflectivity was used for the metallic compounds ($x = 0.18-0.28$). For the in-plane polarization ($\mathbf{E} \perp c$), the parameters in the HR extrapolations $\sigma_{ab}(0)$ are $\sim 1800 \Omega^{-1} \text{cm}^{-1}$ ($x = 0.18$), $\sim 2500 \Omega^{-1} \text{cm}^{-1}$ (0.24), and $\sim 3100 \Omega^{-1} \text{cm}^{-1}$ (0.28), which are roughly in accord with the measured dc values.^{7,11} For the out-of-plane polarization ($\mathbf{E} \parallel c$), systematic data for the dc resistivity $\rho(T)$ have not been reported yet. However, a preliminary measurement at $x = 0.28$ gives $\sigma_c^{\text{dc}} \sim 20-200 \Omega^{-1} \text{cm}^{-1}$ at room temperature.⁷ The $\sigma_c(0)$ obtained in the HR extrapolations are within this range. Variation of the extrapolation procedures had negligible effects on $\sigma(\omega)$ above 0.01 eV for $\mathbf{E} \perp c$ and above 0.02 eV for $\mathbf{E} \parallel c$. R_c in the far-IR region is rather low and hence the connection with the HR reflectivity is not so smooth as for R_{ab} . This reduces to some extent the energy range with sufficiently accurate $\sigma(\omega)$ for $\mathbf{E} \parallel c$ compared with $\mathbf{E} \perp c$.

We also calculate the integrated spectral weight defined by

$$N_{\text{eff}}(\omega) = \frac{2m_0V}{\pi e^2} \int_0^\omega \sigma(\omega') d\omega' \quad (1)$$

(m_0 is the bare-electron mass; V is the unit-cell volume). This represents the effective density of carriers contributing to optical excitations below a certain cutoff energy $\hbar\omega$.

III. RESULTS

A. Spectra of undoped BaCoS₂

Figure 1 shows the reflectivity spectra of BaCoS₂ at room temperature (295 K) on a logarithmic energy scale (0.01–40 eV) for both polarizations, parallel ($\mathbf{E} \perp c$, solid line) and perpendicular ($\mathbf{E} \parallel c$, dashed line) to the CoS plane. The overall features are common to other perovskite-related materials such as the parent compounds of high- T_c cuprates.^{18,19} The spectrum can be separated into three parts, the 0–5 eV, 5–10 eV, and 10–40 eV regions. The highest-energy part is characterized by an edge at ~ 25 eV and ω^{-4} -like decay above that. This edge is the so-called valence-electron plasma edge, which originates from the excitations involving all the valence electrons $N_v = 19$ ($6 \times 2 \text{ S } 3p$ and $7 \text{ Co } 3d$ electrons) (inset of Fig. 1). The middle band starting from 5 eV is assigned to the interband excitations from S $3p$ valence bands to Ba $5d/4f$ conduction bands in the BaS block

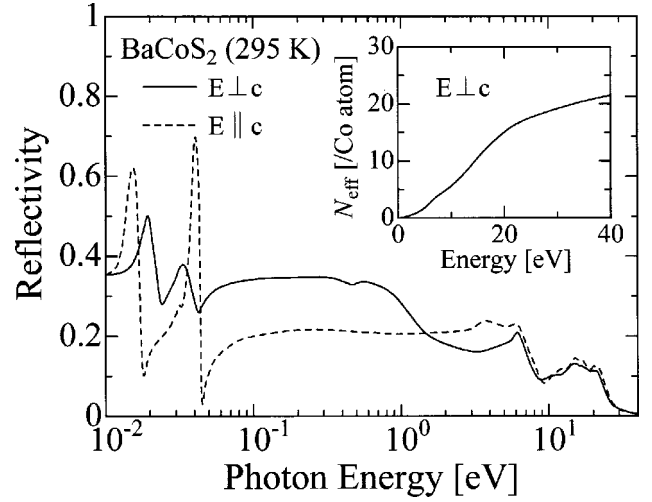


FIG. 1. Optical reflectivity spectra of BaCoS₂ at 295 K for the in-plane ($\mathbf{E} \perp c$, solid line) and out-of-plane ($\mathbf{E} \parallel c$, dashed line) polarizations up to 40 eV. Inset shows the integrated spectral weight N_{eff} for the in-plane electronic contribution. On this energy scale, the out-of-plane contribution is almost the same as the in-plane contribution.

layer.²⁰ These two parts do not exhibit remarkable anisotropy or variation with Ni substitution. The lowest part below 5 eV is dominated by excitations in the CoS plane.

In the lowest-energy region, the spectra of both polarizations show the typical behavior of an insulator, characterized by peaks due to optical phonons in the far-IR region in $R(\omega)$ (Fig. 1) and by gaplike behavior in $\sigma(\omega)$ (Fig. 2). Since the suppression of $\sigma(\omega)$ extends over a wide energy range (~ 1.0 eV and ~ 3.5 eV for the in-plane and out-of-plane polarizations, respectively), it must be an electronic correlation effect, not a localization effect due to disorder or phonons. Another characteristic feature is the anisotropy in $\sigma(\omega)$. These anisotropic optical gaps are explained as charge-transfer (CT) excitations; the 1 eV structure in

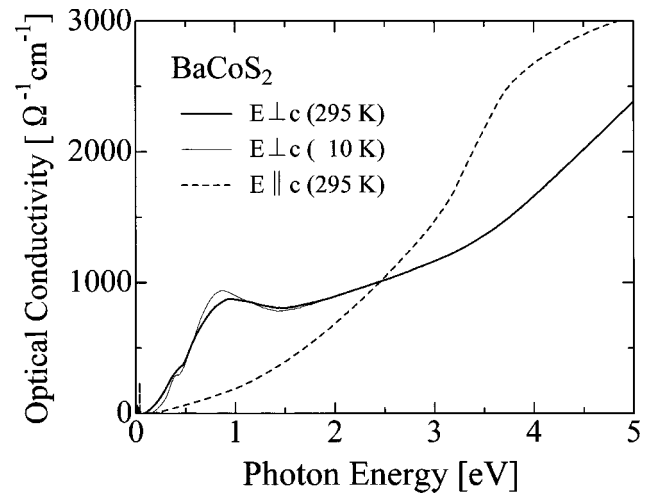


FIG. 2. Optical conductivity spectra of BaCoS₂ deduced from the reflectivity spectra via the Kramers-Kronig transformation for the polarization $\mathbf{E} \perp c$ (295 K, solid line; 10 K, thin line) and $\mathbf{E} \parallel c$ (295 K, dashed line).

$\sigma_{ab}(\omega)$ can be assigned to the planar $S(2) 3p_{\sigma} \rightarrow \text{Co } 3d_{x^2-y^2}$ excitation and the 3.5 eV structure in $\sigma_c(\omega)$ to the apical $S(1) 3p_{\sigma} \rightarrow \text{Co } 3d_{3z^2-r^2}$ excitation. Both are allowed for the $(3d)^7$ configuration of Co^{2+} in BaCoS_2 . In various Co compounds, the on-site $d-d$ Coulomb repulsion energy U is estimated to be at least 4 eV,²¹ and hence BaCoS_2 is classified as a CT-type Mott insulator in the Zaanen-Sawatzky-Allen scheme.^{22,23} In addition, because the out-of-plane gap is larger than the in-plane gap by more than 2 eV, the Co $3d_{3z^2-r^2}$ orbital is suggested to be higher in energy than the Co $3d_{x^2-y^2}$ orbital.

These experimental results on undoped BaCoS_2 contrast with the band calculations,⁵ which predicted a metallic (or semimetallic) state with the configuration $(3d_{3z^2-r^2})^2(3d_{x^2-y^2})^1\bar{L}$ (\bar{L} is a ligand hole) mixed with $(3d_{3z^2-r^2})^2$. This is because the electronic correlation is not appropriately taken into account in the band calculations. Concerning the discrepancy in the order of the energy levels between $3d_{3z^2-r^2}$ and $3d_{x^2-y^2}$, the monoclinic distortion and/or the much longer planar $S(2)$ -Co bond length (~ 2.44 Å) compared with the apical $S(1)$ -Co bond length (~ 2.28 Å) may also play some role.

A weak structure at ~ 0.5 eV in $\sigma_{ab}(\omega)$ might be reminiscent of the $S(2) 3p_{\pi} \rightarrow \text{Co } 3d_{xy,yz,zx}$ excitation. Neutron scattering studies indicate that BaCoS_2 is in the high-spin state with the $(t_{2g})^5(3d_{3z^2-r^2})^1(3d_{x^2-y^2})^1$ configuration,²⁶⁻²⁸ where $S(2) 3p_{\pi} \rightarrow \text{Co } 3d_{xy,yz,zx}$ and $S(1) 3p_{\pi} \rightarrow \text{Co } 3d_{yz,zx}$ excitations are allowed for the in-plane and out-of-plane polarizations, respectively. The tail in $\sigma_c(\omega)$ below the CT excitation at ~ 3.5 eV may be partly explained as the latter CT excitations. Weak $d-d$ transitions, which are expected to be optically active and to have some spectral weight because of the $d-p$ hybridization, may also contribute to the tail.

For the in-plane polarization, the optical phonons are somewhat damped (Fig. 1) and the residual spectral weight persists below the gap at 295 K (solid line in Fig. 2). The indistinct gap structure does not originate from the thermal smearing effect because the low- T (10 K) spectrum shows similar behavior (thin line in Fig. 2). These features suggest that the CT (Mott) gap is closing. The carriers might be slightly doped onto the CoS plane due to the residual sulfur deficiency or the CT gap in BaCoS_2 might have the tendency to close even for the stoichiometric compound. In addition, the indistinct gap structure may also originate from the weak $d-d$ transitions.

B. Ni-substitution effect on the optical spectra

The reflectivity data measured on $\text{BaCo}_{1-x}\text{Ni}_x\text{S}_2$ at 295 K and the KK-transformed conductivity spectra are shown in Fig. 3 and Fig. 4, respectively. The essential change induced by the Ni substitution is the crossover from insulating to metallic spectra. However, the process is different for the two polarizations.

For the in-plane polarization, as the Ni substitution proceeds, a reflectivity edge at about 1 eV appears, although its position does not change much, and the damping of optical phonons becomes intense. For $x \geq 0.18$, the optical phonons

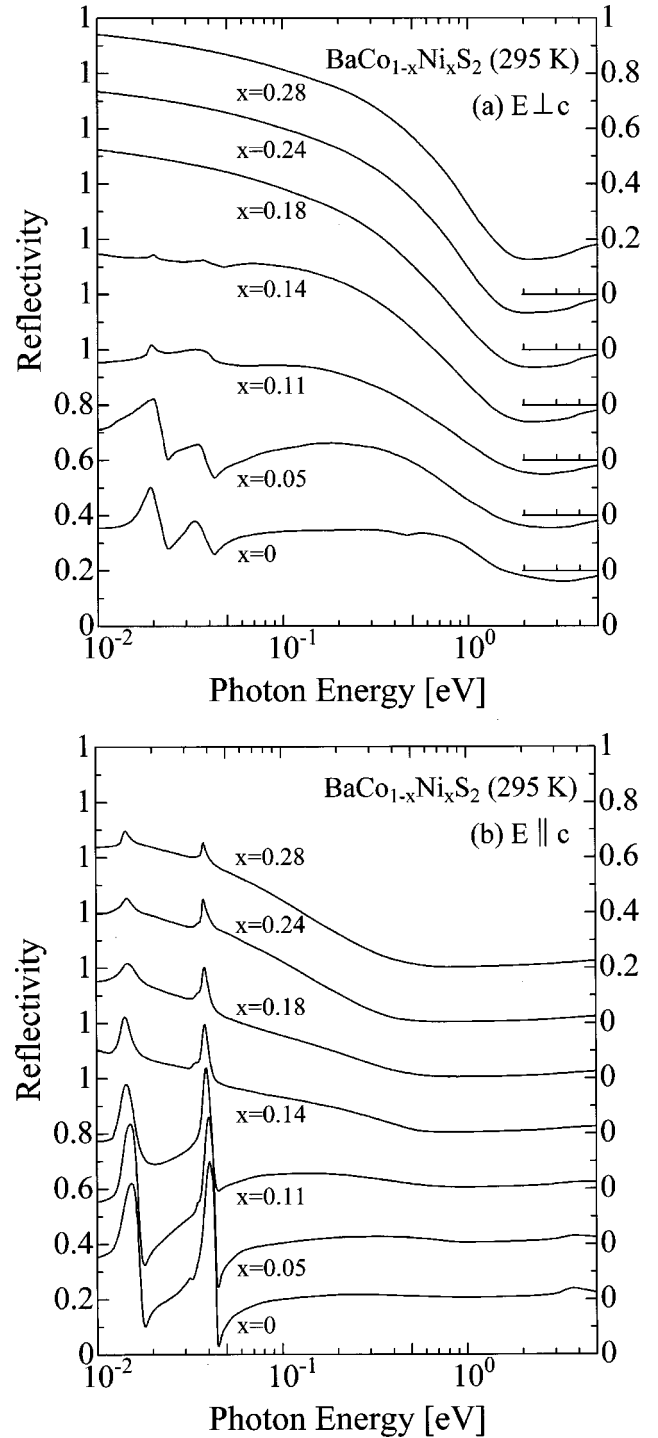


FIG. 3. Optical reflectivity spectra of $\text{BaCo}_{1-x}\text{Ni}_x\text{S}_2$ ($0 \leq x \leq 0.28$) at 295 K for the polarization (a) $E \perp c$ and (b) $E \parallel c$. The curves are shifted upward with increasing Ni content.

are almost completely screened out and the spectrum is solely characterized by the reflectivity edge. According to the change in $R_{ab}(\omega)$ on Ni substitution, a part of the spectral weight in $\sigma_{ab}(\omega)$ from 1 to 5 eV is transferred to the lower-energy region and forms a Drude-like ($\omega=0$ centered) structure in the metallic phase ($x \geq 0.18$). These results are consistent with resistivity studies on single crystals;¹¹ $\rho_{ab}(T)$

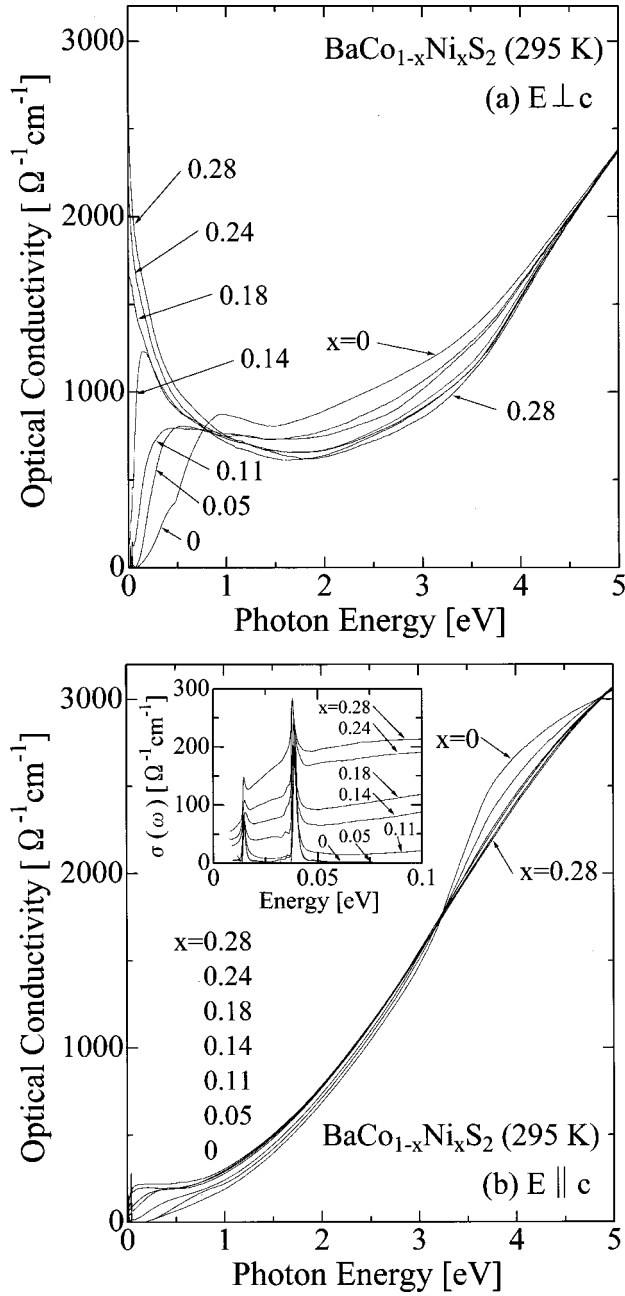


FIG. 4. Optical conductivity spectra of $\text{BaCo}_{1-x}\text{Ni}_x\text{S}_2$ ($0 \leq x \leq 0.28$) deduced from the reflectivity spectra via the Kramers-Kronig transformation for the polarization (a) $\mathbf{E} \perp c$ and (b) $\mathbf{E} \parallel c$. Inset of (b) shows magnified optical conductivity spectra for $\mathbf{E} \parallel c$ in the low-energy region (0–0.1 eV).

is insulating for $x < 0.16$ while it is metallic above T_N (~ 180 K) for $x \sim 0.16$ – 0.22 and over the whole T range for $x > 0.22$.

Variation in $\sigma(\omega)$ over such a wide energy range indicates the reconstruction of the electronic states involving both conduction and valence bands of the parent insulating material, which is commonly observed in the I-M transition of doped Mott insulators.^{19,29–32} The Drude-like term in $\sigma_{ab}(\omega)$ for the metallic compounds is expressed by a slowly decaying feature (roughly, $\sigma \propto \omega^{-1}$) with large energy width

(about 1 eV) rather than a simple Drude formula $\sigma^{\text{dc}}\gamma^2/(\omega^2 + \gamma^2)$ (γ is the damping rate). This is also a common feature in strongly correlated, or Mott-gap-collapsed, metals.^{33–35}

The substitution effect on the optical spectrum is smaller for $\mathbf{E} \parallel c$ than for $\mathbf{E} \perp c$. For the out-of-plane polarization, the optical phonons are less screened and persist up to $x = 0.28$. As the Ni substitution proceeds, the CT structure (~ 3.5 eV) in $\sigma_c(\omega)$ gradually decreases. The missing spectral weight of the CT excitation is transferred to the lower-energy region and forms a broad, mid-IR structure, which gradually develops and shifts downward as x increases. However, a Drude-like component is not confirmed even for the metallic phase where $\sigma_{ab}(\omega)$ shows the Drude-like response. Such anisotropic spectra reflect the 2D electronic structure of $\text{BaCo}_{1-x}\text{Ni}_x\text{S}_2$.

The previous optical study by Kim *et al.* reported that the Drude-like term is limited within the narrow energy region below 0.01 eV with extremely small spectral weight in the $\text{BaCo}_{0.9}\text{Ni}_{0.1}\text{S}_{1.9}$ polycrystal.¹⁶ This seems incompatible with the present result, in which the slowly decaying Drude-like term in $\sigma_{ab}(\omega)$ is much wider. This discrepancy may originate from the large anisotropy between the in-plane and out-of-plane spectra. The reflectivity measured by Kim *et al.* is rather low compared with our $R_{ab}(\omega)$ spectra for the metallic compounds. That low reflectivity may be reproduced by superimposition of the higher in-plane and the lower out-of-plane reflectivity. One should also note that scattering at the grain boundaries and/or the holes may decrease the measured reflectivity in polycrystalline samples.

IV. DISCUSSION

A. Reconstruction of electronic states

The Ni-induced Mott transition in BaCoS_2 is considered to be driven by electron doping onto the $\text{Co}_{1-x}\text{Ni}_x\text{S}$ plane, while the pressure-induced transition is considered to be driven by increase of the transfer energy.¹⁰ The present optical study cannot distinguish these two types of Mott transition. However, it is certain that the present study is incompatible with electron doping in the sense of the rigid band picture. In the rigid band picture, the gap structure at high energy persists with Ni substitution and a Drude term with spectral weight associated with the doped carriers appears at lower energy around 0 eV. This is contrary to the present experimental result, in which $\sigma(\omega)$ varies over a wide energy range up to 5 eV. This feature reflects the restoration process from the strongly correlated CT insulator to the normal semimetal predicted by the band calculations.

This drastic reconstruction seems to occur within the narrow compositional range $x \leq 0.2$. The x-ray absorption spectra do not change appreciably with Ni substitution in the metallic region $x \geq 0.2$.³⁶ After the Mott gap closes, the electronic structure may not be so different from that predicted by the band calculations and hence the rigid band picture may be applicable.³⁷

Substitution of an element in the conducting plane with the same valence (in the present case, Ni^{2+}) corresponds to ‘‘impurity’’ doping in high- T_c cuprates.³⁸ Therefore, one

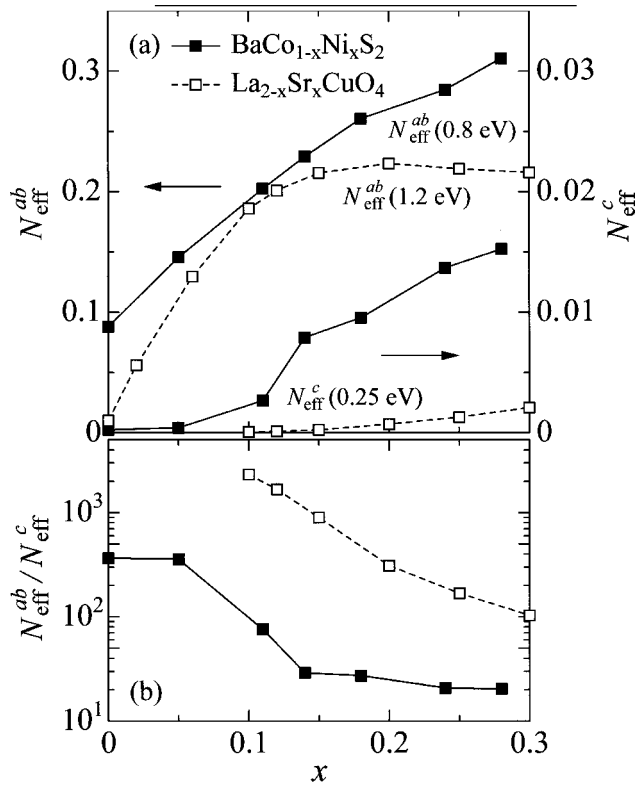


FIG. 5. (a) Integrated spectral weight of the in-plane ($N_{\text{eff}}^{\text{ab}}$) and out-of-plane ($N_{\text{eff}}^{\text{c}}$) electronic contributions plotted against x in $\text{BaCo}_{1-x}\text{Ni}_x\text{S}_2$ (solid squares). Data for $\text{La}_{2-x}\text{Sr}_x\text{CuO}_4$ taken from Refs. 19 and 41 (open squares) are also shown for comparison. The contribution from the optical phonons is subtracted. (b) Anisotropic ratio $N_{\text{eff}}^{\text{ab}}/N_{\text{eff}}^{\text{c}}$ deduced from the N_{eff} data shown in (a).

may doubt whether the substituted Ni really donates a d electron onto the $\text{Co}_{1-x}\text{Ni}_x\text{S}$ plane. However, it is known that the I-M transition in $\text{Ni}_{1-x}\text{Co}_x\text{S}_2$ is caused by the isovalent substitution of Co^{+2} for Ni^{2+} and the mechanism of hole doping by Co substitution has been proposed.³⁹ In addition, a recent study by angle-resolved photoemission spectroscopy (ARPES) suggests mixing between the Co $3d$ and Ni $3d$ orbitals.⁴⁰ The difference between the oxides and the sulfides may be due to the difference in the p orbitals of the anion partner, $2p$ or $3p$.

B. Anisotropy

The highly 2D charge dynamics shown by the present experiment is contrary to the band calculations, which predict a less anisotropic, 3D-like metallic state.⁵ The highly 2D nature is also characteristic of high- T_c cuprates. However, there is a difference between these two systems in the out-of-plane conduction.

The difference is clearly shown by the following plots. In Fig. 5(a), the effective carrier numbers defined by Eq. (1) for the in-plane ($N_{\text{eff}}^{\text{ab}}$) and out-of-plane ($N_{\text{eff}}^{\text{c}}$) polarizations are plotted against x for $\text{BaCo}_{1-x}\text{Ni}_x\text{S}_2$ (solid squares) and for a typical high- T_c cuprate $\text{La}_{2-x}\text{Sr}_x\text{CuO}_4$ (open squares, Refs. 19 and 41). N_{eff} is defined as the number of carriers per Co(Ni) or Cu atom. The contribution from the optical

phonons is subtracted. Figure 5(b) shows the anisotropic ratio $N_{\text{eff}}^{\text{ab}}/N_{\text{eff}}^{\text{c}}$ deduced from these N_{eff} data. Here, the cutoff energy in Eq. (1) is chosen so that we can well approximate the spectral weight of the low-energy electronic excitations. For $N_{\text{eff}}^{\text{ab}}$, it is tuned to the isosbestic point in $\sigma_{\text{ab}}(\omega)$ (0.8 eV for $\text{BaCo}_{1-x}\text{Ni}_x\text{S}_2$ and 1.2 eV for $\text{La}_{2-x}\text{Sr}_x\text{CuO}_4$). For $N_{\text{eff}}^{\text{c}}$, the cutoff energy 0.25 eV corresponds to the energy of the dip in $\sigma_{\text{c}}(\omega)$ of $\text{La}_{2-x}\text{Sr}_x\text{CuO}_4$.⁴¹ Such a dip is not observed in $\text{BaCo}_{1-x}\text{Ni}_x\text{S}_2$, but we chose the same cutoff energy (0.25 eV) for comparison with $\text{La}_{2-x}\text{Sr}_x\text{CuO}_4$. In any case, some variation in the cutoff energy does not affect the general features. In $\text{BaCo}_{1-x}\text{Ni}_x\text{S}_2$, a much larger spectral weight is induced in $\sigma_{\text{c}}(\omega)$ with increasing x than in $\text{La}_{2-x}\text{Sr}_x\text{CuO}_4$. In addition, $N_{\text{eff}}^{\text{c}}$ exhibits a steep rise at smaller x in $\text{BaCo}_{1-x}\text{Ni}_x\text{S}_2$ than in $\text{La}_{2-x}\text{Sr}_x\text{CuO}_4$. This is due to the mid-IR absorption band in $\sigma_{\text{c}}(\omega)$, which is absent in $\text{La}_{2-x}\text{Sr}_x\text{CuO}_4$.

The difference in the out-of-plane charge response may be more clearly shown in dc transport or free-carrier dynamics. In high- T_c cuprates, over a wide compositional range of the superconducting phase, especially in the under- to optimal-doped region, $\rho_{\text{c}}(T)$ is insulating even though $\rho_{\text{ab}}(T)$ is metallic.⁴² This striking feature is a consequence of the ‘‘charge confinement’’ within the plane and has been considered as a possible indication of the non-Fermi-liquid nature of the CuO_2 plane.⁴¹ In high- T_c cuprates, the anisotropic dc conduction does not originate from an anisotropic effective mass m^* (or Drude weight $D^* \sim n/m^*$) but from the unconventional conduction mechanism—coherent in-plane but incoherent out-of-plane conduction.^{41,42} However, previous measurement in $\text{BaCo}_{1-x}\text{Ni}_x\text{S}_2$ shows that $\rho_{\text{c}}(T)$ is metallic and the resistivity anisotropy ratio $\rho_{\text{c}}(T)/\rho_{\text{ab}}(T)$ depends little on temperature.⁷ This suggests that the 2D dc conduction in $\text{BaCo}_{1-x}\text{Ni}_x\text{S}_2$ can result from the anisotropy in m^* (or D^*). That is, the c -axis transport in $\text{BaCo}_{1-x}\text{Ni}_x\text{S}_2$ seems still to be coherent. Although the Drude-like response in $\sigma_{\text{c}}(\omega)$ is not confirmed in the present experiment [inset of Fig. 4(b)], it is possibly hidden by the predominant mid-IR absorption. At $x=0.28$, for example, $\sigma_{\text{c}}(\omega)$ is about $150 \Omega^{-1} \text{cm}^{-1}$ at 0.02 eV, which is larger than (or at least comparable with) the dc conductivity value suggested by the above mentioned $\rho_{\text{c}}(T)$ measurement.⁷ Therefore, our prediction seems to be consistent with the transport study.

The difference in 2D conduction probably originates from a strong interlayer-coupling effect via the $3d_{3z^2-r^2}$ orbital, which loosens the charge confinement even for the slightly doped region and restores coherent c -axis transport. The role of the $3d_{3z^2-r^2}$ orbital is confirmed also by the recent ARPES study.⁴⁰ In contrast, in the high- T_c cuprates, the carriers do not enter the c -axis oriented $3d_{3z^2-r^2}$ orbital,⁴³ and coherent c -axis transport is forbidden, until the carriers are heavily doped. $\text{BaCo}_{1-x}\text{Ni}_x\text{S}_2$ is much more 2D than predicted by the band calculations because of the electronic correlation, but seems to be less 2D than the high- T_c cuprates in this sense. The loose vs tight charge confinement is a significant difference between $\text{BaCo}_{1-x}\text{Ni}_x\text{S}_2$ and high- T_c cuprates.⁴⁴

V. SUMMARY

We have presented optical spectra of $\text{BaCo}_{1-x}\text{Ni}_x\text{S}_2$ single crystals over wide compositional ($0 \leq x \leq 0.28$) and energy ($0.005 \leq \hbar\omega \leq 40$ eV) ranges for both in-plane ($\mathbf{E} \perp c$) and out-of-plane ($\mathbf{E} \parallel c$) polarizations. The spectral features and thus characterized electronic states and structure of $\text{BaCo}_{1-x}\text{Ni}_x\text{S}_2$ are summarized as follows.

(1) The parent compound BaCoS_2 is a charge-transfer-type Mott insulator characterized by an anisotropic optical gap of about (or less than) 1 eV and 3.5 eV for the in-plane and out-of-plane polarizations, respectively.

(2) Ni substitution considerably alters the optical spectra over a wide energy range up to 5 eV. This is incompatible with the rigid band picture and indicates the reconstruction of the electronic states at the Mott transition.

(3) The present optical spectra show the 2D nature of $\text{BaCo}_{1-x}\text{Ni}_x\text{S}_2$. A Drude-like component is not confirmed in $\sigma_c(\omega)$ in the present study even for the metallic phase where $\sigma_{ab}(\omega)$ shows a Drude-like response.

(4) However, the strong interlayer coupling loosens the charge confinement within the plane in $\text{BaCo}_{1-x}\text{Ni}_x\text{S}_2$. The IR spectral weight in $\sigma_c(\omega)$ increases with doping much faster than in high- T_c cuprates and also the c -axis transport remains coherent. The looseness of the confinement may be one of the reasons why $\text{BaCo}_{1-x}\text{Ni}_x\text{S}_2$ does not show superconductivity although it shares many common properties with high- T_c cuprates.

The present study demonstrates that the out-of-plane charge dynamics provides useful information on the electronic states and structure of a 2D doped Mott insulator, because the out-of-plane dynamics clearly and sensitively reflects the character of the orbitals in the vicinity of the Fermi level.

ACKNOWLEDGMENTS

We would like to thank N. Yamane, R. Shiozaki, Y. Sawaki, Y. Moritomo, A. Nakamura, M. Kamada, and M. Hasumoto for their help in the optical measurements. This work was financially supported by a Grant-in-Aid for Scientific Research from the Ministry of Education, Science, and Culture of Japan and by CREST of JST.

*Electronic address: k46291a@nucc.cc.nagoya-u.ac.jp

†Present address: Department of Applied Physics, Tohoku University, Sendai 980-8579, Japan.

¹I. E. Grey and H. Steinfink, *J. Am. Chem. Soc.* **92**, 5093 (1970).

²L. S. Martinson, J. W. Schweitzer, and N. C. Baenziger, *Phys. Rev. Lett.* **71**, 125 (1993); *Phys. Rev. B* **54**, 11 265 (1996).

³G. Jeffrey Snyder, Maria C. Gelabert, and F. J. DiSalvo, *J. Solid State Chem.* **113**, 355 (1994).

⁴B. Fisher, J. Genossar, L. Patlagan, G. M. Reisner, and A. Knizhnik, *Phys. Rev. B* **59**, 8745 (1999).

⁵L. F. Mattheiss, *Solid State Commun.* **93**, 879 (1995); I. Hase, N. Shirakawa, and Y. Nishihara, *J. Phys. Soc. Jpn.* **64**, 2533 (1995).

⁶J. Takeda, K. Kodama, H. Harashina, and M. Sato, *J. Phys. Soc. Jpn.* **63**, 3564 (1994); J. Takeda, Y. Kobayashi, K. Kodama, H. Harashina, and M. Sato, *ibid.* **64**, 2550 (1995).

⁷S. Shamoto, S. Tanaka, E. Ueda, and M. Sato, *J. Cryst. Growth* **154**, 197 (1995).

⁸S. Shamoto, K. Kodama, H. Harashina, M. Sato, and K. Kakurai, *J. Phys. Soc. Jpn.* **66**, 1138 (1997).

⁹H. Sasaki, H. Harashina, K. Kodama, S. Shamoto, M. Sato, K. Kakurai, and M. Nishi, *J. Phys. Soc. Jpn.* **66**, 3975 (1997).

¹⁰H. Sasaki, H. Harashina, K. Kodama, M. Sato, S. Shamoto, M. Nishi, and K. Kakurai, *J. Phys. Soc. Jpn.* **67**, 4235 (1998).

¹¹Y. Yasui, H. Sasaki, S. Shamoto, and M. Sato, *J. Phys. Soc. Jpn.* **66**, 3194 (1997); Y. Yasui, H. Sasaki, M. Sato, M. Ohashi, Y. Sekine, C. Murayama, and N. Mōri, *ibid.* **68**, 1313 (1999).

¹²M. Sato, H. Sasaki, H. Harashina, Y. Yasui, J. Takeda, K. Kodama, S. Shamoto, K. Kakurai, and M. Nishi, *Rev. High Pressure Sci. Technol.* **7**, 447 (1998).

¹³I. Felner, J. Gersten, S. Litvin, U. Asaf, and T. Krōner, *Phys. Rev. B* **52**, 10 097 (1995).

¹⁴C. Looney, J. S. Schilling, L. S. Martinson, and J. W. Schweitzer, *Phys. Rev. Lett.* **76**, 4789 (1996).

¹⁵S. A. M. Mentink, T. E. Mason, B. Fisher, J. Genossar, L. Patlagan, A. Kanigel, M. D. Lumsden, and B. D. Gaulin, *Phys. Rev. B* **55**, 12 375 (1997).

¹⁶K. H. Kim, Y. H. Kim, L. S. Martinson, and J. W. Schweitzer, *Phys. Rev. Lett.* **78**, 4498 (1997).

¹⁷S. Shamoto, S. Tanaka, E. Ueda, and M. Sato, *Physica C* **263**, 550 (1996).

¹⁸S. Tajima, H. Ishii, T. Nakahashi, H. Takagi, S. Uchida, M. Seki, S. Suga, Y. Hidaka, M. Suzuki, T. Murakami, K. Oka, and H. Unoki, *J. Opt. Soc. Am. B* **6**, 475 (1989).

¹⁹S. Uchida, T. Ido, H. Takagi, T. Arima, Y. Tokura, and S. Tajima, *Phys. Rev. B* **43**, 7942 (1991).

²⁰Y. Kaneko, K. Morimoto, and T. Koda, *J. Phys. Soc. Jpn.* **52**, 4385 (1983).

²¹A. E. Bocquet, T. Mizokawa, T. Saitoh, H. Namatame, and A. Fujimori, *Phys. Rev. B* **46**, 3771 (1992).

²²J. Zaanen, G. A. Sawatzky, and J. W. Allen, *Phys. Rev. Lett.* **55**, 418 (1985).

²³D. D. Vvedensky, in *Unoccupied Electronic States*, edited by J. C. Fuggle and J. E. Inglesfield (Springer-Verlag, Berlin, 1992), p. 139.

²⁴N. C. Baenziger, L. Grout, L. S. Martinson, and J. W. Schweitzer, *Acta Crystallogr., Sect. C: Cryst. Struct. Commun.* **50**, 1375 (1994).

²⁵K. Kodama, H. Fujishita, H. Harashina, S. Taniguchi, J. Takeda, and M. Sato, *J. Phys. Soc. Jpn.* **64**, 2069 (1995).

²⁶K. Kodama, S. Shamoto, H. Harashina, J. Takeda, M. Sato, K. Kakurai, and M. Nishi, *J. Phys. Soc. Jpn.* **65**, 1782 (1996).

²⁷D. Mandrus, J. L. Sarrao, B. C. Chakoumakos, J. A. Fernandez-Baca, S. E. Nagler, and B. C. Sales, *J. Appl. Phys.* **81**, 4620 (1997).

²⁸Y. Yasui, H. Sasaki, M. Sato, M. Ohashi, Y. Sekine, C. Murayama, and N. Mōri, *Physica B* **281&282**, 625 (2000).

²⁹J. Orenstein, G. A. Thomas, A. J. Millis, S. L. Cooper, D. H. Rapkine, T. Timusk, L. F. Schneemeyer, and J. V. Waszczak, *Phys. Rev. B* **42**, 6342 (1990).

³⁰T. Ido, K. Magoshi, H. Eisaki, and S. Uchida, *Phys. Rev. B* **44**, 12 094 (1991).

³¹S. L. Cooper, D. Reznik, A. Kotz, M. A. Karlow, R. Liu, M. V. Klein, W. C. Lee, J. Giapintzakis, D. M. Ginsberg, B. W. Veal, and A. P. Paulikas, *Phys. Rev. B* **47**, 8233 (1993).

- ³²Y. Taguchi, Y. Tokura, T. Arima, and F. Inaba, *Phys. Rev. B* **48**, 511 (1993).
- ³³S. Uchida, H. Eisaki, and S. Tajima, *Physica B* **186-188**, 975 (1993).
- ³⁴P. Kostic, Y. Okada, N. C. Collins, Z. Schlesinger, J. W. Reiner, L. Klein, A. Kapitulnik, T. H. Geballe, and M. R. Beasley, *Phys. Rev. Lett.* **81**, 2498 (1998).
- ³⁵K. Takenaka, Y. Sawaki, and S. Sugai, *Phys. Rev. B* **60**, 13 011 (1999).
- ³⁶E. Z. Kurmaev, Y. M. Yarmoshenko, M. Neumann, S. Stadler, D. L. Ederer, I. Hase, A. Fujimori, M. Sato, Y. Yasui, R. C. C. Perera, M. M. Grush, T. A. Callcott, D. A. Zatsopin, V. A. Trofimova, and V. V. Sokolov, *J. Phys. Chem. Solids* **59**, 1459 (1998).
- ³⁷The physical properties of the highly Ni-doped metallic phase are not incompatible with the prediction from the band calculations. (See, for example, Refs. 2 and 26.) This suggests that crossover from the high- to low-spin state as well as reversing of the energy levels between the $3d_{3z^2-r^2}$ and $3d_{x^2-y^2}$ orbitals occur in this x region.
- ³⁸For example, see T. R. Chien, Z. Z. Wang, and N. P. Ong, *Phys. Rev. Lett.* **67**, 2088 (1991).
- ³⁹A. K. Mabatah, E. J. Yoffa, P. C. Eklund, M. S. Dresselhaus, and D. Adler, *Phys. Rev. B* **21**, 1676 (1980).
- ⁴⁰T. Sato, H. Kumigashira, D. Ionel, Y. Naitoh, T. Takahashi, I. Hase, H. Ding, J. C. Campuzano, and S. Shamoto (unpublished).
- ⁴¹For a review, see S. Uchida, K. Tamasaku, and S. Tajima, *Phys. Rev. B* **53**, 14 558 (1996).
- ⁴²For example, see K. Takenaka, K. Mizuhashi, H. Takagi, and S. Uchida, *Phys. Rev. B* **50**, 6534 (1994).
- ⁴³E. Pellegrin, N. Nücker, J. Fink, S. L. Molodtsov, A. Gutiérrez, E. Navas, O. Strebler, Z. Hu, M. Domke, G. Kaindl, S. Uchida, Y. Nakamura, J. Markl, M. Klauda, G. Saemann-Ischenko, A. Krol, J. L. Peng, Z. Y. Li, and R. L. Greene, *Phys. Rev. B* **47**, 3354 (1993).
- ⁴⁴These differences may be summarized as the absence of the “underdoped” region in $\text{BaCo}_{1-x}\text{Ni}_x\text{S}_2$. This is consistent with the fact that $\rho_{ab}(T)$ of metallic $\text{BaCo}_{1-x}\text{Ni}_x\text{S}_2$ exhibits Fermi-liquid-like, T -superlinear behavior (Ref. 6) rather than unconventional T -linear behavior (Ref. 42) even near the Mott transition.